DOI: 10.17725/j.rensit.2024.16.043

Investigation a method for measuring blood pressure with a capacitive integrated sensor

Andrey K. Movchan, Eugeniy V. Lomakov, Eugeniy V. Rogozhnikov, Kirill V. Savenko
Tomsk State University of Control Systems and Radioelectronics, https://tusur.ru/
Tomsk 634050, Russian Federation
E-mail: ltaak@tu.tusur.ru, evgenii.v.lomakov@tusur.ru, evgenii.v.rogozhnikov@tusur.ru, kirill.savenko@tusur.ru

Received October 19, 2023, peer-reviewed October 26, 2023, accepted November 02, 2023, published March 15, 2024.

Abstract: **A method of wireless measurement of blood flow parameters is investigated using an implantable passive capacitive sensor and an external reader. This device is designed to measure the parameters of blood flow in the human body, through the installation of a passive capacitive sensor and inductive coupling with an external reader device. The method of wireless measurement is based on the connection of resonant circuits at an operating frequency of 10 MHz. The mathematical calculation of the device circuit is presented. The result of the calculation was the dependence of the output voltage of the external reader on the change of capacitance in the implanted passive sensor. The values of the potential sensitivity of the device are obtained. The manufactured layout of the device and its parameters are presented. The mock-up allowed to investigate the dependences of the coupling factor of the circuits when using coils of an external reader of different sizes. Also the measurement of the output voltage of the external reader from the value of the passive sensor capacitance was made. The value of real sensitivity of the device layout was measured.**

Keywords: **resonant circuit, passive sensor, blood flow, coupling factor, stent, capacitive sensor**

UDC 621.31

For citation: Andrey K. Movchan, Eugeniy V. Lomakov, Eugeniy V. Rogozhnikov, Kirill V. Savenko. Investigation a method for measuring blood pressure with a capacitive integrated sensor. *RENSIT: Radioelectronics. Nanosystems. Information Technologies,* 2024, 16(1):43-52e. DOI: 10.17725/j.rensit.2024.16.043.

Contents

1. INTRODUCTION

Cardiovascular diseases (CVD) remain the leading form of mortality worldwide, which may affect one in three of us. Atherosclerosis is a progressive form of CVD that is characterised by the imperceptible development of fatty plaques that are caused by proliferation of vascular smooth muscle cells and influx of inflammatory cells and proteins [1]. This leads to narrowing of blood vessels and restricted blood flow, which is responsible for most heart attacks and strokes. The problem remains unresolved despite intensive research and numerous drug trials. The consequences of vasoconstriction often require surgical intervention, one of which is the endoprosthesis of arterial aneurysms with a stent graft. Stent restenosis

may occur despite the successful opening of blood vessels and restoration of blood flow. Stents are developed with the integration of devices that include various sensors, as well as a wireless communication system. This is necessary for early diagnosis of restenosis and monitoring of blood flow in real time. Integrated devices can be categorized into active and passive devices. The advantage of active devices is a high level of functionality, since electronic circuits and power supply devices are integrated together. However, such devices have a disadvantage in the built-in power supply device, which has a limited service life. Consequently, such devices are unsuitable for implantation into the human body or into a blood vessel. Also, active devices can have wireless communication, as described in the article [2]. But in this paper, the simulation is carried out using an optimal current source and complex circuits, which increases the cost of such a sensor. Passive devices do not need a constant power source, but have lower efficiency compared to active ones. Also, passive devices have a lower manufacturing cost. As a rule, an integrated passive device includes a capacitor and an inductor, which can be a conventional inductor or an arterial stent [3].

The integrated passive devices can be designed in a variety of ways. One of the articles under consideration describes an implementation where an external signal source creates a radio frequency field that affects the resonant circuit of a passive device. The passive device has a resonant frequency due to inductance and capacitance. The oscillations at the frequency of the external source are generated during the operation of the passive device in the resonant circuit. Then the external device receives the parameter due to inductive coupling with a passive sensor. The parameter is related to the oscillations that are necessary to evaluate the characteristics of the fluid flow through the stent. Despite the scope of this study, the working distance of the sensor is several millimeters, which is not enough for the sensor to work in the human body [4].

Also, articles [5,6] consider variants of embedded antennas in passive sensors that allow improving the efficiency of wireless transmission of energy and data.

We can conclude that the area of implantable sensors is being actively explored for monitoring blood flow parameters. We have established that methods of early detection of restenosis need further research and development, including integrated sensors and external reader devices.

This work considers the possibility of implementing remote measurement of blood flow parameters due to an integrated passive capacitive sensor that is inductively connected to an external reader device.

2. MEASURING PRINCIPLE

The measurement principle is implemented as follows: the external reader device and the passive sensor are the primary and secondary resonant circuits, which are schematically shown in **Fig. 1.** The primary circuit consists of an inductance L_1 and a capacitor C_1, which form an LC oscillating circuit. The circuit also has a signal generator for generating oscillations with a certain frequency. The secondary circuit includes an inductance L_2 and a variable capacitor C_2, which mimics a capacitive sensor to form an LC-oscillating circuit.

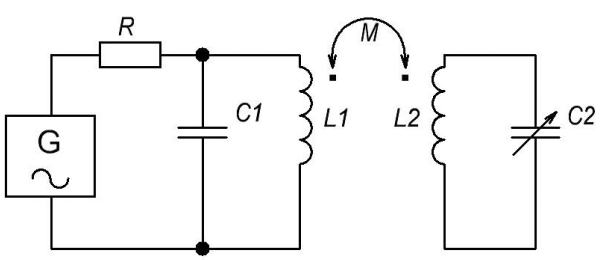

Fig. 1. *Simplified electrical diagram.*

The secondary circuit receives energy from the primary circuit due to their inductive coupling. In this case, the blood flow affects the capacitive sensor, thereby affecting the parameters of the primary circuit due to inductive coupling.

The resonant frequency of a passive device can be expressed as its function of inductance L and capacitance C, as shown in equation (1)

$$\omega_0 = \frac{1}{\sqrt{LC}}. \quad (1)$$

The value of the inductance of the passive device remains constant after manufacture, and the capacitance of the capacitor changes when the parameters of the blood flow change. Accordingly, the resonant frequency of the passive device will also depend on the parameters of the blood flow according to expression (1). Remote determination of the parameters of the internal passive device is realized due to the inductive coupling of the external and internal devices. As a result, the parameters of the integrated sensor affect the parameters of the reader device. This allows to be determined the blood flow parameters on the external device side.

Energy losses during the propagation of radio frequency signals can depend on many parameters, including the resonant frequencies of the two coils and their orientation. If the thickness of the tissue between the external and internal devices is less than one tenth of the wavelength, then the energy absorption is proportional to the square of the signal frequency. Therefore, the operating frequency of the signal cannot be too high. In other words, a system with a high resonant frequency is capable of transmitting a large amount of energy, but this frequency must be reduced due to the increase in energy absorbed by human tissues. On the other hand, high Q-factor are difficult to obtain at low resonant frequencies. Therefore, the resonant frequency should be chosen according to the factors of the device application. In this study, the operating frequency was chosen to be 10 MHz.

High energy transfer efficiency is important in wireless systems where energy is transferred from one coil to another. The high Q-factor allows the oscillating circuit to save energy for a long time. Also, the high Q-factor allows to reduce energy losses and improve transmission efficiency.

The Q-factor of the circuit is determined by the ratio of the characteristic impedance ρ of the oscillating circuit to the internal resistance r of this circuit:

$$Q = \frac{\rho}{r}. \quad (2)$$

The characteristic impedance of the circuit is defined by the formula:

$$\rho = \sqrt{\frac{L}{C}}. \quad (3)$$

The internal resistance of the external circuit is selected 0.1 Ohm, and the required Q-factor is at least 500. The parameters of the oscillatory circuit are obtained equal to L = 800 nH and C = 320 pF based on the condition of the oscillation frequency of the circuit equal to 10 MHz and formula (4):

$$f = \frac{1}{2\pi\sqrt{LC}}. \quad (4)$$

3. MATHEMATICAL MODELING

The idea of a non-contact passive sensor of blood flow parameters investigated in this work is based on inductively coupled resonant circuits, as shown in **Fig. 2**.

The resonant circuit of the integrated part of the sensor is formed by elements L_2, r_2 and the capacitive sensor C_2, and the external circuit of the reader part is formed by elements L_1, r_1, C_1. The equivalent sources e_{21} and e_{12} reflect the mutual electromotive force (EMF) that is induced in each of the circuits due to the action of the inductive coupling. The source E_0 is the energy

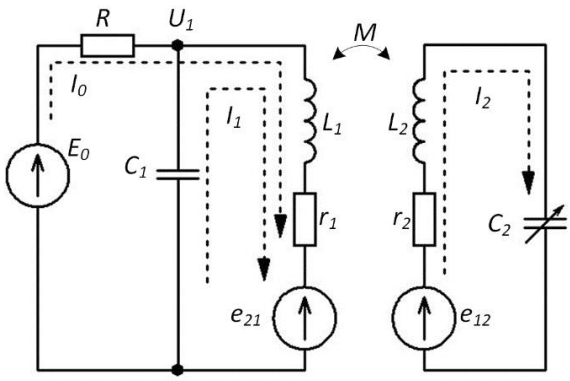

Fig. 2. *Electrical diagram of the sensor.*

source in this circuit and forms a harmonic EMF with a circular frequency ω.

The output parameter of the reader part of the sensor is the voltage U_1 of the external reader circuit. In this case, U_1 is determined by the circuit parameters and, in particular, by the capacitance of the capacitive sensor C_2, which is used in the device for measuring blood flow parameters. The change in the output parameter U_1 can be determined using a linear amplitude detector. The estimate of the potential sensitivity of the sensor is determined from the dependence $U_1(C_2)$, where U_1 is the output voltage of the reader part, C_2 is the capacitance of the capacitive sensor of the integrated part of the device.

$U_1(C_2)$ is determined using the mesh current method [7]. The system of equations of mesh current for the circuit shown in Fig. 2 has the following form:

$$\begin{cases} (R + r_1 + j\omega L_1)I_0 + (r_1 + j\omega L_1)I_1 - e_{21} = E_0, \\ (r_1 + j\omega L_1)I_0 + (r_1 + j\omega L_1 + \dfrac{1}{j\omega C_1})I_1 - e_{21} = 0, \\ (r_2 + j\omega L_2 + \dfrac{1}{j\omega C_2})I_2 - e_{12} = 0. \end{cases} \quad (5)$$

The mutual induction EMFs e_{21} and e_{12} are determined as follows in the respective circuits:

$$e_{21} = j\omega M I_2, \quad (6)$$

$$e_{12} = j\omega M (I_0 + I_1), \quad (7)$$

where M is the mutual inductance of the connected circuits, defined as:

$$M = k\sqrt{L_1 L_2}, \quad (8)$$

where k is the coupling factor of the coupled circuits determined by the mutual configuration of the windings of inductances L_1 and L_2 and the distance between them.

The following substitutions are used to simplify the presentation of the results of solving contour equations (5):

interaction impedance

$$X_M = \omega M, \quad (9)$$

serial impedance of the reader circuit Z_1

$$Z_1 = r_1 + j\omega L_1 + \frac{1}{j\omega C_1}, \quad (10)$$

impedance $L_1 r_1$ of the reader circuit branch Z_{11}

$$Z_{11} = r_1 + j\omega L_1, \quad (11)$$

serial impedance of the integrated circuit Z_2

$$Z_2 = r_2 + j\omega L_2 + \frac{1}{j\omega C_2}. \quad (12)$$

Taking into account the above mentioned substitutions, the system of equations of mesh current for the circuit shown in Fig. 2 will have the following form:

$$\begin{cases} (R + Z_{11})I_0 + Z_{11}I_1 - jX_M I = E_0, \\ Z_{11}I_0 + Z_1 I_1 - jX_M I_2 = 0, \\ Z_2 I_2 - jX_M (I_0 + I_1) = 0. \end{cases} \quad (13)$$

The solution of the system of equations (5) will be expressions for the currents corresponding to the branches of the circuit shown in Fig. 2. In particular, the expression for the current I_0 feeding the reader circuit has the following form:

$$I_0 = \frac{E_0}{R + Z_{11} + \dfrac{X_M^2}{Z_2} - \dfrac{\left(Z_{11} + \dfrac{X_M^2}{Z_2}\right)^2}{Z_1 + \dfrac{X_M^2}{Z_2}}}. \quad (14)$$

In expression (14), the summand $X_M^2 / Z_2 = Z_{ins}$ is the amount of insertion

resistance from the integrated circuit to the readout circuit.

The introduced resistance Z_{ins} is a consequence of the inductive coupling of the circuits and is determined by the magnitude of the coupling factor k and, importantly, the parameters of the integrated circuit.

The expression for the current I_0 will take the following form taking into account the introduced notation Z_{ins}

$$I_0 = \frac{E_0}{R + Z_{11} + Z_{ins} - \frac{(Z_{11} + Z_{ins})^2}{Z_1 + Z_{ins}}}. \quad (15)$$

From equations (13) it is also possible to determine the values of the remaining currents using the current I_0. Thus, the expression for the current I_1 of the read circuit is as follows:

$$I_1 = \frac{Z_{11} + Z_{ins}}{Z_1 + Z_{ins}} I_0. \quad (16)$$

Expression for the current I_2 of the integrated circuit

$$I_2 = \frac{jX_M}{Z_2}(I_0 + I_1). \quad (17)$$

The voltage U_1 on the reader circuit can be obtained as follows:

$$U_1 = E_0 - RI_0. \quad (18)$$

Expression (18) leads to the following result for U_1 taking into account (15):

$$U_1 = E_0 \left[1 - \frac{R}{R + Z_{11} + Z_{ins} - \frac{(Z_{11} + Z_{ins})^2}{Z_1 + Z_{ins}}} \right]. \quad (19)$$

Fig. 3 shows the dependence of the absolute value of the voltage on the reader circuit on the frequency $U_1(f)$. Dependences are plotted for three values of coupling factor k_1 = 0.05, k_2 = 0.01, k_3 = 0.005 and frequency range f from 9.5 MHz to 10.5 MHz. The values of the parameters of the circuit elements (Fig. 2) are as follows: E_0 = 10 *V*, R = 1 kOhm, $L_1 = L_2$ = 800 nH, $C_1 = C_2$ = 320 pF, r_1 = 0.1 Ohm, r_2 = 1 Ohm.

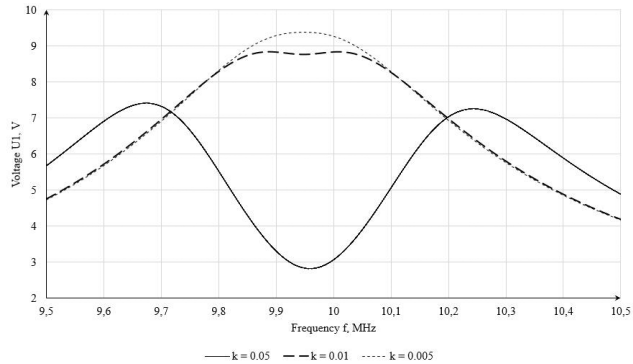

Fig. 3. *The dependence of the absolute value of the voltage on the reading circuit on the frequency.*

The voltage U_1 on the reader circuit and its dependence on the capacitance of the capacitive sensor of the integrated circuit must be determined to assess the potential sensitivity of the sensor.

Fig. 4 shows the dependence of the absolute value of the voltage on the reader circuit on the capacitance value of the sensor of the integrated circuit $U_1(C_2)$.

The dependences are constructed for three values of the coupling factor k_1 = 0.05, k_2 = 0.01, k_3 = 0.005 and the range of variation C_2 from 260 pF to 380 pF. The values of the parameters of the circuit elements (Fig. 2) are as follows: R = 1 kOhm, $L_1 = L_2$ =800 nH, C_1 = 320 pF, r_1 = 0.1 Ohm, r_2 = 1 Ohm, f = 10 MHz.

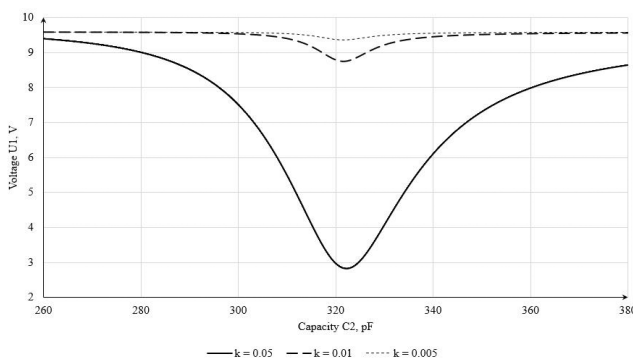

Fig. 4. *Dependences of the absolute value of the voltage on the reading circuit on the capacitance C_2.*

In this case, the potential sensitivity of the sensor is determined by the dependence of the voltage change ΔU_1 on the reader circuit when the capacitance C_2 in the integrated circuit changes by the value ΔC. That is, it is necessary to find the differential of the dependence $U_1(C_2)$:

$$\Delta U_1(C_2) = \frac{\partial}{\partial C_2} U_1(C_2) \cdot \Delta C. \quad (20)$$

Expressions (5) are calculated and dependences $\Delta U_1(C_2)$ are constructed for three values of the coupling factor $k_1 = 0.05$, $k_2 = 0.01$, $k_3 = 0.005$, frequency $f = 10$ MHz, the range of capacitance C_2 from 260 pF to 380 pF and $\Delta C = 1$pF. The remaining parameters of the circuit elements (Fig. 2) are as follows: $R = 1$ kOhm, $L_1 = L_2 = 800$ nH, $C_1 = 320$ pF, $r_1 = 0.1$ Ohm, $r_2 = 1$ Ohm.

Based on the graphs shown in **Fig. 5**, the maximum sensitivity values $\Delta U_1(C_2)$ at $\Delta C = 1$ pF for each of the values of the coupling factor have the following values: for $k_1 = 0.05$, the maximum sensitivity is achieved when the capacitance of the capacitive sensor $C_2 = 310$ pF and is $\Delta U_1(C_2) = -0.237$ V/pF, for $k_2 = 0.01$, when $C_2 = 317$ pF, $\Delta U_1(C_2) = -0.085$ V/pF, and for $k_3 = 0.005$, when $C_2 = 318$ pF, $\Delta U_1(C_2) = -0.024$ V/pF. The minus sign in $\Delta U_1(C_2)$ indicates that as the capacitance of C_2 increases, the voltage U_1 decreases.

The results obtained show that the sensitivity of this meter depends on the coupling factor of the circuits k, i.e. on the mutual configuration

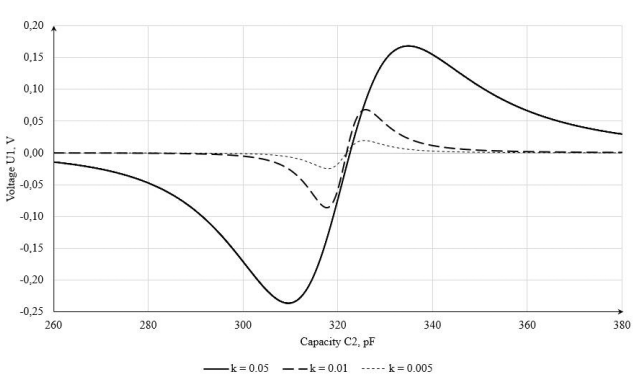

Fig. 5. *Dependences of sensor sensitivity on C_2 capacity.*

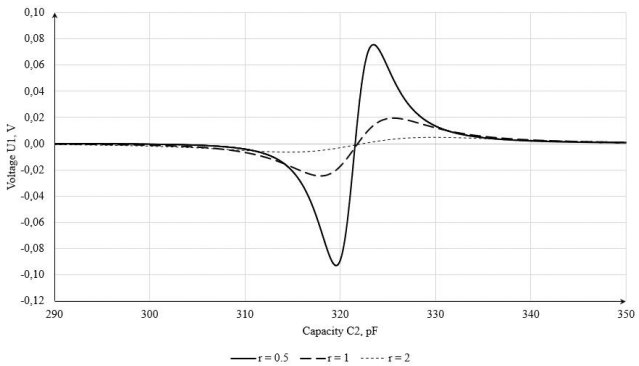

Fig. 6. *Dependences of sensor sensitivity on C_2 capacity.*

of the inductance windings L_1 and L_2 and the distance between them.

Since r_2 to make a small value is a very labour-intensive task in view of the small overall size of the coil L_2, it is of interest to obtain the dependence of the sensor sensitivity on the active loss resistance r_2 in the integrated circuit.

Fig. 6 shows the dependences of the sensor sensitivity $\Delta U_1(C_2)$ for a fixed value of the coupling factor $k = 0.005$ and three values of the loss resistance r_2 in the integrated circuit: $r_2 = 0.5$ Ohm, $r_2 = 0.5$ Ohm and $r_2 = 2$ Ohm. Frequency is $f = 10$ MHz, the range of capacitance C_2 is from 290 pF to 350 pF and $\Delta C = 1$ pF. The remaining parameters of the circuit elements (Fig. 2) are as follows: $R = 1$ kOhm, $L_1 = L_2 = 800$ nH, $C_1 = 320$ pF, $r_1 = 0.1$ Ohm.

Based on the graphs shown in Fig. 6, the maximum sensitivity values $\Delta U_1(C_2)$ at $\Delta C = 1$ pF for each of the loss resistance values r_2 have the following values: for $r_2 = 0.5$ Ohms, the maximum sensitivity is achieved at the capacitance of the capacitive sensor $C_2 = 319$ pF and is $\Delta U_1(C_2) = -0.092$ V/pF, for $r_2 = 1$ Ohm, at $C_2 = 318$ pF, $\Delta U_1(C_2) = -0.02$ V/pF, and for $r_2 = 2$ Ohms, at $C_2 = 314$ pF, $\Delta U_1(C_2) = -0.006$ V/pF.

The results obtained show that the sensitivity of this meter also significantly depends on the loss resistance r_2. At the same time, the active resistance of losses in the L_2 coil of the integrated circuit must be reduced to increase the sensitivity of the device.

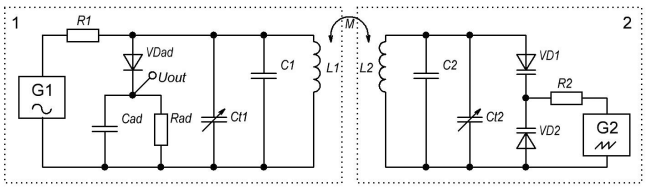

Fig. 7. *Electrical schematic diagram of the layout.*

4. EXPERIMENTAL RESEARCH

The experimental layout was designed and assembled to study the practical implementation of the described method based on the above. **Fig. 7** shows the electrical circuit of the layout, which contains the following components: inductance $L_1 = L_2 =$ 800 nH, constant capacitance $C_1 = C_2 = 300$ pF, variable capacitance $C_{t1} = C_{t2} = 2$-30 pF, resistor $R_1 =$ kOhm, generator of a sinusoidal signal with a frequency $G_1 = 10$ MHz, varicap $VD_1 = VD_2 =$ KB121A, limiting resistor $R_2 = 152$ kOhm, generator of linearly increasing voltage with frequency $G_2 = 2$ Hz, diode $VD_{ad} = 1N4148$, constant capacitance $C_{ad} = 12$ nF, resistor $R_{ad} = 100$ kOhm.

Components L_1, C_1, C_{t1} form the primary oscillating circuit (reader circuit), L_2, C_2, C_{t2} form the secondary oscillating circuit (integrated circuit), VD_{ad}, C_{ad}, R_{ad} form the amplitude detector of the primary circuit, VD_1, VD_2 form the voltage controlled variable capacitance to simulate the operation of the capacitive sensor of the integrated circuit.

Fig. 8 shows the voltage dependence of the capacitance, which is the main characteristic of the voltage-controlled variable capacitance for this device.

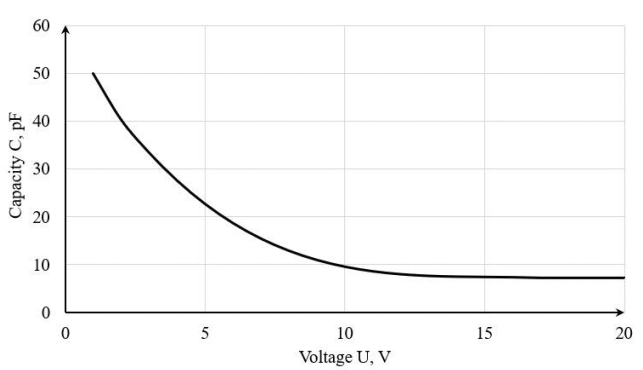

Fig. 8. *Capacitance-voltage curve of the KV121A varicap.*

The pressure-simulating signal can be isolated using an amplitude detector. The amplitude detector is used to isolate the amplitude envelope of a high-frequency radio signal. The calculation of the parameters of the amplitude detector was based on the condition of formula (17) and the parameters of the experimental layout.

$$Xc = \frac{1}{2\pi f \cdot C}. \quad (17)$$

The layout consists of two universal printed circuit boards with a soldered circuit, according to Fig. 7. One of the printed circuit boards is fixed and represents the primary circuit. The secondary circuit is located on a movable printed circuit board, which has the ability to move in the longitudinal axis, thereby making it possible to change the distance between the coils of the primary and secondary circuits. **Fig. 9** shows the assembled layout.

The first stage of the work is to study the dependence of the coupling factor on the form factor of the coils. The coupling factor of inductance determines the degree of mutual inductive coupling between two coils in an electrical circuit. It shows how a change in the current I_1 in one coil affects the induction of voltage U_2 in another coil. The coupling factor depends on the geometry of the coils, the distance between them and other factors. It is assumed that the inductance coil included in the passive device has small overall dimensions due to the limitation that this coil is integrated into a human artery.

It is assumed that the inductance included in the passive device has small overall

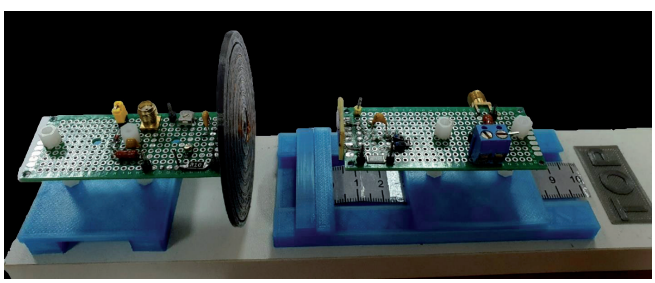

Fig. 9. *Experimental layout.*

dimensions due to the limitation that this coil is integrated into a human artery. Therefore, the form factor of the external reader coil must be changed to achieve a high coupling factor. A flat spiral coil on a printed circuit board was used as an inductance oMf a passive device with the following characteristics: outer diameter D = 15 mm, inner diameter d = 2 mm, printed track width W = 0.035 mm, winding pitch s = 0.6 mm, printed conductor thickness h = 0.035 mm, number of coils turns N = 11, inductance L = 800 nH.

Table 1 shows the parameters of the coils that were used as the inductance of the external device. Coils 1-3 have the shape of a ring, wound turn to turn, coil 4 has the shape of a flat spiral.

Table 1

Parameters of external coils

Coil	D, mm	d, mm	N	L, nH
1	22	10	6.3	760
2	28	20	4.25	720
3	64	60	2.25	760
4	54	10	5	850

All the capacitive elements, as well as the elements of the amplitude detector, were switched off when measuring the coupling factor from the circuit shown in Fig. 7. **Fig. 10** shows the graphs that were obtained as a result of the study of the dependence of the coupling factor on the distance for various external inductance.

The formula for calculating the coupling factor is (18).

$$k = \frac{U_2}{2\pi f I_1 \sqrt{L_1 L_2}}. \quad (18)$$

We can conclude from the data on the graph shown in Fig. 10 that the form factor of the coils affects the coupling factor. Coil 4 is used for further research in the external reader circuit, due to the greater coupling factor at the interval from 10 mm to 40 mm.

The next stage of the work is the measurement of the volt-farad characteristics of the sensor, in accordance with the scheme shown in Fig. 7. A linearly increasing voltage was applied from the generator to the varicap to simulate pressure changes. The magnitude of the amplitude varied in the range according to the volt-farad characteristic of the varicap shown in **Fig. 11**.

The range of capacitance variation is limited by the volt-farad characteristic of the varicap, in this regard, only part of the dependence of the output voltage of the primary circuit on the capacitance value of the capacitive sensor is shown. The curve of the volt-farad characteristic has an asymmetric character based on the graph shown in Fig. 11. This is caused by the difference in the parameters of the primary and secondary circuits, as well as the nonlinear dependence of the varicap capacitance on the applied voltage. The

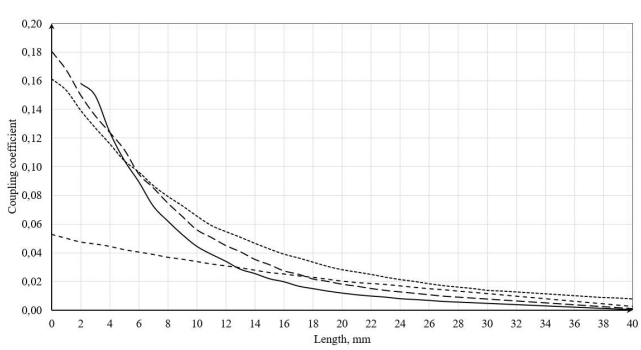

Fig. 10. *Experimental dependences of the coupling factor on the distance.*

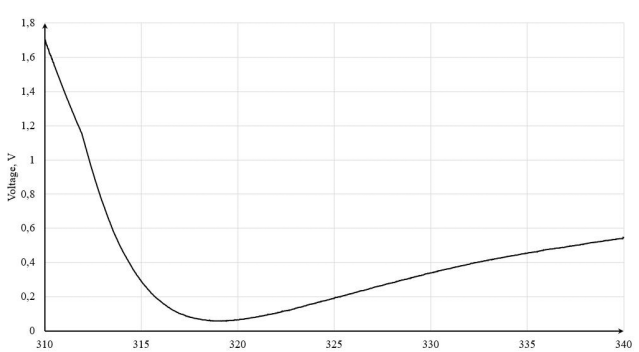

Fig. 11. *Experimental capacitance-voltage curve of the sensor.*

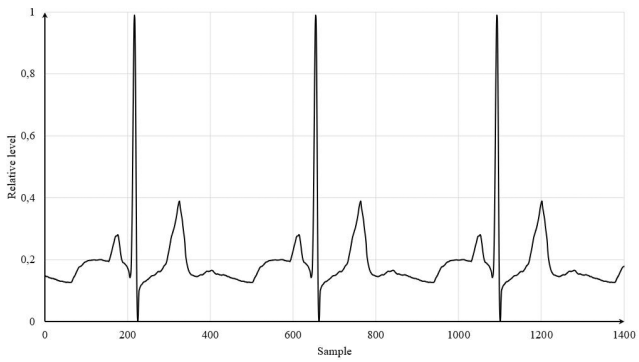

Fig. 12. *Cardioimpulse.*

maximum value of the real sensitivity $\Delta U_1(C_2)$ was 30 mV/pF.

Further simulations of blood pressure changes were performed using a G_2 generator connected to the secondary circuit. **Fig. 12** shows samples of the cardiac pulse signal that was generated by the G_2 generator. This signal, having 438 samples per pulse, with a frequency of 2 Hz was applied to the varicaps (Fig. 7), thereby changing the total capacity of the secondary circuit. **Fig. 13** shows factorgram at the output of the linear amplitude detector of the reader device.

The graph of the output signal of the reader circuit has some differences from the signal loaded into the generator G_2, due to the nonlinearity of varicaps, the difference of parameters of both circuits, and the small number of samples per pulse. The nonlinearity of the sensor can be compensated by calibrating the device.

Fig. 13. *The output signal of the reader circuit.*

5. CONCLUSION

This work deals with a method of wirelessly measuring blood flow parameters using an implantable passive sensor and reader device. This study performs a mathematical calculation of the electrical circuit of the measuring device, which resulted in the dependence of the output voltage of the reader device on the change of capacitance in the implanted sensor. The potential sensitivity of the measuring device is calculated based on the obtained dependencies for the specified parameters. The potential sensitivity was $\Delta U_1(C_2) = -0.085$ V/pF with a contour coupling factor $k = 0.01$.

Next, the manufactured layout was presented and its parameters were given. The dependence of the coupling factor of the circuits was studied for different dimensions of the primary circuit coils on this layout. The coupling factor was $k = 0.008$ when using a spiral coil with a diameter of 54 mm of the primary circuit and a coil of a secondary circuit with a diameter of 15 mm at a distance of 40 mm based on the results obtained. Next, the dependence of the output voltage of the reader device on the change in the capacitance of the secondary circuit was measured. The capacitance of the secondary circuit was changed by a linear change in the voltage on the varicap. The real sensitivity of the measurement device layout was estimated and amounted to 0.03 V/pF at a distance between the coils of 35 mm, which corresponds to the coupling factor $k \approx 0.011$. The difference between the potential and real sensitivity of the measuring device is caused by the difference in the parameters of the primary and secondary circuits, as well as the nonlinear dependence of the varicap capacitance on voltage.

An experiment was also performed in which a voltage was applied to the varicaps in the form of a cardioimpulse. As a result, the amplitude detector of the external reader device showed a distorted cardio pulse signal, reflecting the nonlinearity of the measurement device. The

study showed a strong dependence of the output parameter of the device on the distance between the external reader and the implantable sensor and the size of the coils of the contours, as well as on the losses in the contour of the implantable sensor.

The study showed a strong dependence of the output parameter of the device on the distance between the external reader and the implanted sensor and the size of the coils of the circuits, as well as on the losses in the circuit of the implanted sensor. Despite this, the method of measuring blood flow parameters presented in this paper can be used in practice with appropriate calibration.

REFERENCES

1. World Health Organization: Cardiovascular Diseases (CVDs), June 11 2021, accessed: Oct. 1 2023, available: https://www.who.int/news-room/fact-sheets/detail/cardiovascular-diseases-(cvds)
2. Yakovlev A, Kim S, Poon A. Implantable biomedical devices: Wireless powering and communication. *IEEE Communications Magazine,* 2012, 50(4):152-159.
3. Bussooa A, Neale S, Mercer JR. Future of smart cardiovascular implants. *Sensors,* 2018, 18(7):2008.
4. Park J, Kim JK, Patil SJ, Park JK, Park S, Lee DW. A Wireless Pressure Sensor Integrated with a Biodegradable Polymer Stent for Biomedical Applications. *Sensors*, 2016, 16:809.
5. Zhang J, Das R, Abbasi QN, Mirzai N, Mercer J, Heidari H. Dual-band Microstrip Patch Antenna for Fully-Wireless Smart Stent. *IEEE: International Symposium on Antennas and Propagation and USNC-URSI Radio Science Meeting* (*APS/URSI*), 2021, p. 1035-1036.
6. Chen SC, Zhang ZY, Liu CH. Stent-Based Antennas for Smart Stent Applications. *IEEE: International Symposium on Antennas and Propagation* (*ISAP*), 2018, p. 1-2.
7. Yorke R. *Electric Circuit Theory: Applied Electricity and Electronics.* Oxford, Pergamon Press, 1981, 350 p.